Novel Hybrid Precoding Designs for mmWave Multiuser Systems with Partial Channel Knowledge

Yahia R. Ramadan, *Student Member*, *IEEE*, and Hlaing Minn, *Fellow*, *IEEE*
Electrical and Computer Engineering Department, University of Texas at Dallas, Richardson, TX, 75080, USA
Email: {yahia.ramadan, hlaing.minn}@utdallas.edu

***Abstract*—Millimeter-wave (mmWave) large-scale antenna systems typically apply hybrid analog-digital precoders to reduce hardware complexity and power consumption. In this paper, we design the hybrid precoder to maximize the average sum rate of mmWave multiuser downlink systems with partial channel knowledge in contrast to the full channel knowledge assumption of the existing approaches. We design the zero-forcing (ZF) hybrid precoder with partial channel knowledge, and provide the necessary conditions for its application. If these conditions are not satisfied, we propose another hybrid precoder design which is based on the signal-to-interference-and-noise ratio (SINR) and signal-to-leakage-and-noise ratio (SLNR). Performance results corroborate advantages of the proposed hybrid precoder designs over a benchmark design.**

***Index Terms*—Millimeter wave, hybrid precoding, multiuser, partial channel knowledge, sum rate.**

I. Introduction

Next generation wireless communication systems demand an exponential increase in data rate. The spectrum available in the microwave band is too scarce to answer such data rate need. This leads to a potential use of the underutilized millimeter-wave (mmWave) band. Millimeter-wave communications can support multiple Gbps data rates, but since the carrier frequencies are so high, mmWave links suffer higher propagation path loss. Antenna arrays can be used to compensate such losses [1]. Tens of antennas can be packed into a small area in mmWave transceivers due to the tiny wavelength. However, implementing a separate radio-frequency (RF) chain for each antenna is impractical due to the high cost and power of mixed-signal devices. An efficient solution to reduce the hardware complexity and the power consumption is the hybrid analog-digital precoding, where the antenna array with $N_{\rm T}$ elements is connected via an analog RF precoder to $N_{\rm RF}$ RF chains ($K \leq N_{\rm RF} < N_{\rm T}$) which process the digitally-precoded transmitted streams for K users [2].

The existing hybrid precoder designs for mmWave systems can be divided into two categories. In the first category, it is assumed that the transmitter has full channel knowledge before designing the hybrid precoder. For a single user, it was shown that by minimizing the average Euclidean distance between the fully digital precoder and the hybrid precoder, the hybrid precoder can achieve performance very close to that of the fully digital precoding [3]–[5]. For multiple users, a two-stage hybrid precoder design was developed in [6], [7]. At the first stage, the transmitter and the users jointly select (using a feedback from the users) the best pair of RF precoder and RF combiner to maximize the channel gain. Then, the baseband precoder is designed as a zero-forcing (ZF) precoder for the equivalent channels. In [8], the hybrid precoder design was enhanced by minimizing the mean-squared error (MSE) of the transmitted data streams. In the second category, it is assumed that the transmitter has knowledge of the second-order channel statistics [9]–[11]. Using the second-order channel statistics, the transmitter designs the RF precoder. Then, the transmitter estimates the equivalent channel based on which the baseband precoder is designed as a ZF precoder.

We note that most of previous works assume full channel knowledge at the transmitter either before designing the hybrid precoder (the first category) or after designing the RF precoder (the second category). On the contrary, the assumption of partial channel knowledge at the transmitter, where the transmitter has knowledge of the angles of departure (AoDs) of the propagation paths only, is more practical. Since the AoDs are invariant with frequency in time-division duplex (TDD) or frequency-division duplex (FDD) operation mode, the transmitter does not need any feedback [9], [12], [13]. Moreover, the variation of the AoDs is slower than the variation of the channel gains that makes it possible to use the same hybrid precoder for multiple symbols. This paper designs the hybrid precoder to maximize the average sum rate of mmWave multiuser downlink systems with partial channel knowledge in contrast to the full channel knowledge assumption of the existing approaches.

Our contributions can be summarized as follows. 1) We design the ZF hybrid precoder with partial channel knowledge if $N_{\rm T} > (K-1)L$ and $N_{\rm RF} \geq 2K$, where L is the number of propagation paths per user. 2) If these conditions are not satisfied, we propose another hybrid precoder design that is based on signal-to-interference-and-noise ratio (SINR) and signal-to-leakage-and-noise ratio (SLNR). We derive closed-form expressions for the average SINR and SLNR. Using a lower bound on SLNR, we obtain the baseband precoder as a function of the RF precoder. Then, we propose a simple gradient ascent algorithm which designs the RF precoder using the gradient of the closed-form SLNR. To ensure the convergence, we update the RF precoder to maximize the average sum rate obtained using the closed-form SINR. 3) Since the hybrid precoder design with partial channel knowledge for multiple users has not been discussed in the literature, we develop the closed-form Eigenvector-SLNR (EV-SLNR) hybrid precoder (based on previous works with some modifications) which we consider as our benchmark design. 4) We present sum-rate characteristics of the proposed hybrid precoders with partial channel knowledge under different values of $N_{\rm RF}$ and SNR.

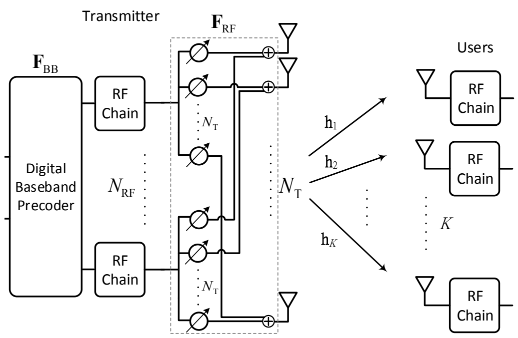

Fig. 1. mmWave multiuser system with K single-antenna users.

We use the following notation throughout this paper: $\mathbf{A}$ is a matrix, $\|\mathbf{A}\|_{\rm F}$ is its Frobenius norm, $\mathbf{a}$ is a vector, $\|\mathbf{a}\|$ is its $l2$-norm, and a is a scalar, whereas $(\cdot)^T$and $(\cdot)^H$ are the transpose and conjugate transpose operators respectively. $\mathbf{I}_N$ is the identity matrix of order N. $\mathrm{Tr}\left[\mathbf{A}\right]$ denotes the trace of $\mathbf{A}$, $\boldsymbol{\mathcal{E}}_{\max}\left[\mathbf{A}\right]$ is the principal eigenvector of $\mathbf{A}$, and $\lambda_{\max}\left[\mathbf{A}\right]$ is the corresponding maximum eigenvalue. $\mathcal{N}\left[\mathbf{A}\right]$ returns the orthonormal basis of the null space of $\mathbf{A}$. $\mathrm{diag}\left(a_1,a_2,\ldots,a_N\right)$ returns the diagonal concatenation of elements $a_1,a_2,\ldots,a_N$. $\mathbb{P}\left(x\right)$ and $\mathbb{E}\left(x\right)$ denote the probability and expectation of x. $\mathbf{A}\left(i:j,:\right)$ consists of the $i^{\rm th}$ to the $j^{\rm th}$ rows of $\mathbf{A}$, while $\mathbf{A}\left(:,i:j\right)$ consists of the $i^{\rm th}$ to the $j^{\rm th}$ columns of $\mathbf{A}$.

The rest of this paper is organized as follows. In section II, we describe the system and the channel models. In section III, we present the proposed ZF hybrid precoder. In section IV, we introduce the proposed SINR-SLNR hybrid precoder. In section V, we develop the EV-SLNR hybrid precoder. In section VI, we present the numerical results. Finally, section VII concludes the paper.

II. System and Channel Models

A. System Model

We consider a mmWave multiuser downlink system with K single-antenna users as shown in Fig. 1. The transmitter is equipped with a uniform linear array (ULA) with $N_{\rm T}$ antennas. The spacing between antennas is half the wavelength. To reduce the hardware complexity and the power consumption, the uniform linear antenna array is connected via an analog RF precoder to $N_{\rm RF}$ RF chains ($K\leq N_{\rm RF}<N_{\rm T}$) which process the digitally-precoded streams.

We consider a narrow-band transmission, where the received signal y_k at the $k^{\rm th}$ user is given by

$$y_k=\mathbf{h}_k\mathbf{F}_{\rm RF}\mathbf{f}_{{\rm BB},k}s_k+\sum_{\substack{i=1\\ i\neq k}}^{K}\mathbf{h}_k\mathbf{F}_{\rm RF}\mathbf{f}_{{\rm BB},i}s_i+z_k, \qquad (1)$$

where $\mathbf{h}_k\in\mathbb{C}^{1\times N_{\rm T}}$ is the mmWave channel to the $k^{\rm th}$ user, $\mathbf{F}_{\rm RF}\in\mathbb{C}^{N_{\rm T}\times N_{\rm RF}}$ is the analog RF precoder, $\mathbf{f}_{{\rm BB},k}\in\mathbb{C}^{N_{\rm RF}\times 1}$ is the digital baseband precoder for the $k^{\rm th}$ user, s_k is the transmitted modulated symbol to the $k^{\rm th}$ user with $\mathbb{E}\left[|s_k|^2\right]=P$, and z_k is the zero-mean additive white complex Gaussian noise with variance σ^2 at the $k^{\rm th}$ user. The RF precoder $\mathbf{F}_{\rm RF}$ and the baseband precoder $\mathbf{F}_{\rm BB}=\left[\mathbf{f}_{{\rm BB},1},\mathbf{f}_{{\rm BB},2},\ldots,\mathbf{f}_{{\rm BB},K}\right]\in\mathbb{C}^{N_{\rm RF}\times K}$ have to be designed jointly due to the coupled power constraint $\|\mathbf{F}_{\rm RF}\mathbf{F}_{\rm BB}\|_{\rm F}^2=K$. The analog RF preocder $\mathbf{F}_{\rm RF}$ is usually implemented using analog phase shifters and analog combiners. We consider the fully-connected structure which requires $N_{\rm T}N_{\rm RF}$ analog phase shifters and $N_{\rm T}$ analog combiners. Therefore, we have the constraint that $\left|\mathbf{F}_{\rm RF}\left(m,n\right)\right|=1\,\forall m,n$.

B. Channel Model

Millimeter-wave channels are expected to have limited scattering [14], [15]. Therefore, we adopt a sparse geometric multipath channel model, where the channel vector $\mathbf{h}_k$ to the $k^{\rm th}$ user is given by

$$\mathbf{h}_k=\sqrt{\frac{N_{\rm T}}{L}}\sum_{l=1}^{L}\alpha_{l,k}\mathbf{a}_{l,k}^H, \qquad (2)$$

where L is the number of propagation paths, $\alpha_{l,k}$ is the channel gain of the $l^{\rm th}$ path to the $k^{\rm th}$ user, $\mathbf{a}_{l,k}$ is the transmit steering vectors of the $l^{\rm th}$ path to the $k^{\rm th}$ user with azimuth angle of departure (AoD) of $\varphi_{l,k}$, and

$$\mathbf{a}_{l,k}=\frac{1}{\sqrt{N_{\rm T}}}\left[1,e^{-j\pi\cos(\varphi_{l,k})},\ldots,e^{-j\pi(N_{\rm T}-1)\cos(\varphi_{l,k})}\right]^T. \qquad (3)$$

Let $\mathbf{A}_{{\rm T},k}\in\mathbb{C}^{N_{\rm T}\times L}$ be the transmit array response matrix to the $k^{\rm th}$ user given by

$$\mathbf{A}_{{\rm T},k}=\left[\mathbf{a}_{1,k},\mathbf{a}_{2,k},\ldots,\mathbf{a}_{L,k}\right]. \qquad (4)$$

Since each resolvable path consists of several paths, similar to [16, Section III-E], the channel gains $\{\alpha_{l,k}\}$ are assumed to be independent complex Gaussian random variables with zero-mean and unit variance.

Throughout the paper, we assume partial channel knowledge at the transmitter, where the transmitter has knowledge of only the AoDs of the propagation paths. Since the AoDs are invariant with frequency in TDD or FDD operation mode, the transmitter does not need any feedback [9], [12], [13]. Moreover, the variation of the AoDs is slower than the variation of the channel gains that makes it possible to use the same hybrid precoder for multiple symbols.

C. Hybrid Precoding Design Problem

The achievable rate R_k of the $k^{\rm th}$ user is given by

$$R_k=\log_2\left(1+\frac{\left|\mathbf{h}_k\mathbf{F}_{\rm RF}\mathbf{f}_{{\rm BB},k}\right|^2}{\sum_{\substack{i=1\\ i\neq k}}^{K}\left|\mathbf{h}_k\mathbf{F}_{\rm RF}\mathbf{f}_{{\rm BB},i}\right|^2+\delta}\right), \qquad (5)$$

where $\delta=1/\gamma$ and $\gamma=P/\sigma^2$ is the transmit SNR per user. Our aim is to maximize the average sum rate $R_{\rm sum}$ given by

$$R_{\rm sum}=\sum_{k=1}^{K}\mathbb{E}\left[\log_2\left(1+\frac{\left|\mathbf{h}_k\mathbf{F}_{\rm RF}\mathbf{f}_{{\rm BB},k}\right|^2}{\sum_{\substack{i=1\\ i\neq k}}^{K}\left|\mathbf{h}_k\mathbf{F}_{\rm RF}\mathbf{f}_{{\rm BB},i}\right|^2+\delta}\right)\right], \qquad (6)$$

where the expectation is performed only over the unknown channel gains $\{\alpha_{l,k}\}$. Using Jensen's inequality, we have

$$R_{\rm sum}\leq\sum_{k=1}^{K}\log_2\left(1+\overline{\rm SINR}_k\right)\triangleq R_{\rm sum}^{\rm UB}, \qquad (7)$$

where $\overline{\rm SINR}_k=\mathbb{E}\left[\frac{\left|\mathbf{h}_k\mathbf{F}_{\rm RF}\mathbf{f}_{{\rm BB},k}\right|^2}{\sum_{\substack{i=1\\ i\neq k}}^{K}\left|\mathbf{h}_k\mathbf{F}_{\rm RF}\mathbf{f}_{{\rm BB},i}\right|^2+\delta}\right]$ is the average receive SINR of the $k^{\rm th}$ user. Alternatively, we design the hybrid precoder to maximize the average sum rate upper bound $R_{\rm sum}^{\rm UB}$,

$$\begin{aligned}\left[\mathbf{F}_{\rm RF},\mathbf{F}_{\rm BB}\right] &= \underset{\mathbf{F}_{\rm RF},\mathbf{F}_{\rm BB}}{\arg\max}\,R_{\rm sum}^{\rm UB},\\ &\quad \text{s.t.}\quad \left|\mathbf{F}_{\rm RF}\left(m,n\right)\right|=1\,\forall m,n,\\ &\qquad\quad \|\mathbf{F}_{\rm RF}\mathbf{F}_{\rm BB}\|_{\rm F}^2=K. \end{aligned} \qquad (8)$$

Next, we propose different hybrid precoding designs to maximize the average sum rate upper bound $R_{\rm sum}^{\rm UB}$.

III. Proposed Zero-Forcing Hybrid Precoder

The zero-forcing (ZF) hybrid precoder is designed to null the interference to each user. With full channel knowledge, the baseband precoder is used to null the interference to each user [6], [7]. As a result, it is only necessary that $N_{\mathrm{RF}} \geq K$ to apply the ZF precoder with full channel knowledge. On the other hand, with partial channel knowledge, using the baseband precoder to null the interference to each user requires that $N_{\mathrm{RF}} > (K-1)L$ since it is necessary to null L directions for each one of the $K-1$ interfering users. However, the condition $N_{\mathrm{RF}} > (K-1)L$ is not likely to be satisfied in mmWave systems due to the high cost and power of RF chains. Alternatively, we use the RF precoder to null the interference to each user. Therefore, we obtain a simpler condition on N_{RF} (as will be shown).

Dropping the unit modulus constraint, let $\mathbf{f}_k$ be the precoder for the k^{th} user. We express $\mathbf{f}_k$ as

$$\mathbf{f}_k = \mathbf{U}_k \tilde{\mathbf{f}}_k, \tag{9}$$

where $\mathbf{U}_k = \mathcal{N}\left[\mathbf{A}_{\mathrm{T},1}, \ldots, \mathbf{A}_{\mathrm{T},k-1}, \mathbf{A}_{\mathrm{T},k+1}, \ldots, \mathbf{A}_{\mathrm{T},K}\right] \in \mathbb{C}^{N_{\mathrm{T}} \times (N_{\mathrm{T}}-(K-1)L)}$ is a semi-unitary matrix in the null space of the directions to the $K-1$ interfering users, and $\tilde{\mathbf{f}}_k \in \mathbb{C}^{(N_{\mathrm{T}}-(K-1)L)\times 1}$. Therefore, it is necessary that $N_{\mathrm{T}} > (K-1)L$. We design $\tilde{\mathbf{f}}_k$ to maximize the expected receive SNR of the k^{th} user ($\overline{\mathrm{SNR}}_k$) given by

$$\begin{aligned}\overline{\mathrm{SNR}}_k &= \mathbb{E}\left[\gamma \left|\mathbf{h}_k \mathbf{U}_k \tilde{\mathbf{f}}_k\right|^2\right] \\ &= \frac{\gamma N_{\mathrm{T}}}{L} \tilde{\mathbf{f}}_k^H \mathbf{U}_k^H \left(\sum_{l=1}^{L} \mathbf{a}_{l,k} \mathbb{E}\left[|\alpha_{l,k}|^2\right] \mathbf{a}_{l,k}^H\right) \mathbf{U}_k \tilde{\mathbf{f}}_k \\ &= \frac{\gamma N_{\mathrm{T}}}{L} \tilde{\mathbf{f}}_k^H \mathbf{U}_k^H \left(\sum_{l=1}^{L} \mathbf{a}_{l,k} \mathbf{a}_{l,k}^H\right) \mathbf{U}_k \tilde{\mathbf{f}}_k. \end{aligned} \tag{10}$$

By maximizing $\overline{\mathrm{SNR}}_k$ with the constraint $\|\mathbf{f}_k\|^2 = 1$, we obtain $\tilde{\mathbf{f}}_k$ as

$$\tilde{\mathbf{f}}_k = \boldsymbol{\mathcal{E}}_{\max}\left[\mathbf{U}_k^H \left(\sum_{l=1}^{L} \mathbf{a}_{l,k} \mathbf{a}_{l,k}^H\right) \mathbf{U}_k\right], \tag{11}$$

and the corresponding $R_{\mathrm{sum,ZF}}^{\mathrm{UB}}$ is expressed as

$$R_{\mathrm{sum,ZF}}^{\mathrm{UB}} = \sum_{k=1}^{K} \log_2\left(1 + \frac{\gamma N_{\mathrm{T}}}{L} \lambda_{\max}\left[\mathbf{U}_k^H \left(\sum_{l=1}^{L} \mathbf{a}_{l,k} \mathbf{a}_{l,k}^H\right) \mathbf{U}_k\right]\right). \tag{12}$$

Therefore, the precoder matrix $\mathbf{F}$ is expressed as $\mathbf{F} = [\mathbf{f}_1, \mathbf{f}_2, \ldots, \mathbf{f}_K] \in \mathbb{C}^{N_{\mathrm{T}} \times K}$. However, the precoder matrix $\mathbf{F}$ is not likely to satisfy the unit modulus constraint. In [17], it was shown that any vector $\mathbf{x} \in \mathbb{C}^{N \times 1}$ can be expressed as $\mathbf{x} = \tilde{\mathbf{X}}\tilde{\mathbf{x}}$, where $\tilde{\mathbf{X}} \in \mathbb{C}^{N \times 2}$ is with unit modulus entries and $\tilde{\mathbf{x}} \in \mathbb{R}^{2\times 1}$. Following this decomposition, we decompose $\mathbf{F}$ as $\mathbf{F} = \mathbf{Q}_{\mathrm{RF}} \mathbf{R}_{\mathrm{BB}}$, where $\mathbf{Q}_{\mathrm{RF}} \in \mathbb{C}^{N_{\mathrm{T}} \times 2K}$ is with unit modulus entries, and $\mathbf{R}_{\mathrm{BB}} \in \mathbb{R}^{2K \times K}$. Therefore, it is also necessary that $N_{\mathrm{RF}} \geq 2K$ to apply the ZF hybrid precoder by setting $\mathbf{F}_{\mathrm{RF}}(:, 1:2K) = \mathbf{Q}_{\mathrm{RF}}$ and $\mathbf{F}_{\mathrm{BB}}(1:2K, :) = \mathbf{R}_{\mathrm{BB}}$. In conclusion, with partial channel knowledge, it is necessary that $N_{\mathrm{T}} > (K-1)L$ and $N_{\mathrm{RF}} \geq 2K$ to apply the ZF hybrid precoder.

IV. Proposed SINR-SLNR Hybrid Precoder

If the conditions $N_{\mathrm{T}} > (K-1)L$ and/ or $N_{\mathrm{RF}} \geq 2K$ are not satisfied, the zero-forcing hybrid precoder is infeasible. Therefore, we propose another hybrid precoder design that is based on SINR and SLNR. Let $\overline{\mathrm{SINR}}_k$ and $\overline{\mathrm{SLNR}}_k$ be the expected receive SINR and SLNR of the k^{th} user respectively. Next, we drive closed-form expressions for $\overline{\mathrm{SINR}}_k$ and $\overline{\mathrm{SLNR}}_k$. Then, we use both $\overline{\mathrm{SINR}}_k$ and $\overline{\mathrm{SLNR}}_k$ to maximize $R_{\mathrm{sum}}^{\mathrm{UB}}$.

A. A Closed-Form Expression for SINR

The average receive SINR of the k^{th} user $\overline{\mathrm{SINR}}_k$ is given by

$$\overline{\mathrm{SINR}}_k = \mathbb{E}\left[\frac{\left|\mathbf{h}_k \mathbf{F}_{\mathrm{RF}} \mathbf{f}_{\mathrm{BB},k}\right|^2}{\sum_{\substack{i=1\\ i\neq k}}^{K} \left|\mathbf{h}_k \mathbf{F}_{\mathrm{RF}} \mathbf{f}_{\mathrm{BB},i}\right|^2 + \delta}\right]. \tag{13}$$

It can be rewritten as

$$\overline{\mathrm{SINR}}_k = \mathbb{E}\left[\frac{\boldsymbol{\alpha}_k^H \mathbf{A}_k \boldsymbol{\alpha}_k}{\boldsymbol{\alpha}_k^H \mathbf{B}_k \boldsymbol{\alpha}_k + \tilde{\delta}}\right], \tag{14}$$

where $\boldsymbol{\alpha}_k = \left[\alpha_{1,k}, \alpha_{2,k}, \ldots, \alpha_{L,k}\right]^T$, $\mathbf{A}_k = \mathbf{A}_{\mathrm{T},k}^H \mathbf{F}_{\mathrm{RF}} \mathbf{f}_{\mathrm{BB},k} \mathbf{f}_{\mathrm{BB},k}^H \mathbf{F}_{\mathrm{RF}}^H \mathbf{A}_{\mathrm{T},k}$, $\mathbf{B}_k = \mathbf{A}_{\mathrm{T},k}^H \mathbf{F}_{\mathrm{RF}} \left(\sum_{\substack{i=1\\ i\neq k}}^{K} \mathbf{f}_{\mathrm{BB},i} \mathbf{f}_{\mathrm{BB},i}^H\right) \mathbf{F}_{\mathrm{RF}}^H \mathbf{A}_{\mathrm{T},k}$, and $\tilde{\delta} = \frac{L}{\gamma N_{\mathrm{T}}}$. We can notice that $\overline{\mathrm{SINR}}_k$ in (14) is the expected value of a ratio of quadratic forms of $\boldsymbol{\alpha}_k$. Moreover, $\boldsymbol{\alpha}_k$ is a circularly-symmetric complex Gaussian random vector with a probability density function (PDF) $f_{\boldsymbol{\alpha}_k}(\boldsymbol{\alpha}_k)$ given by [18]

$$f_{\boldsymbol{\alpha}_k}(\boldsymbol{\alpha}_k) = \frac{e^{-\boldsymbol{\alpha}_k^H \boldsymbol{\alpha}_k}}{\pi^L}. \tag{15}$$

Let w_1 and w_2 be two random variables such that $\mathbb{P}(w_2 > 0) = 1$. In [19], it was shown that

$$\mathbb{E}\left[\frac{w_1}{w_2}\right] = \int_0^{\infty} \left[\frac{\partial}{\partial s} M_{w_1,w_2}(s, -r)\right]_{s=0} dr, \tag{16}$$

where $M_{w_1,w_2}(s, r)$ is the joint moment generating function of w_1 and w_2. Define $w_1 = \boldsymbol{\alpha}_k^H \mathbf{A}_k \boldsymbol{\alpha}_k$ and $w_2 = \boldsymbol{\alpha}_k^H \mathbf{B}_k \boldsymbol{\alpha}_k + \tilde{\delta}$, we obtain $M_{w_1,w_2}(s, -r)$ as

$$\begin{aligned} M_{w_1,w_2}(s,-r) &= \int_{-\infty}^{\infty} \pi^{-L} e^{-\boldsymbol{\alpha}_k^H \boldsymbol{\alpha}_k} e^{\boldsymbol{\alpha}_k^H \mathbf{A}_k \boldsymbol{\alpha}_k s - \boldsymbol{\alpha}_k^H \mathbf{B}_k \boldsymbol{\alpha}_k r - \tilde{\delta} r} d\boldsymbol{\alpha}_k \\ &= e^{-\tilde{\delta} r} \left|\mathbf{I}_L - \mathbf{A}_k s + \mathbf{B}_k r\right|^{-1}. \end{aligned} \tag{17}$$

Therefore, we can evaluate $\overline{\mathrm{SINR}}_k$ as

$$\begin{aligned} \overline{\mathrm{SINR}}_k &= \int_0^{\infty} \left[\frac{\partial}{\partial s} e^{-\tilde{\delta} r} \left|\mathbf{I}_L - \mathbf{A}_k s + \mathbf{B}_k r\right|^{-1}\right]_{s=0} dr \\ &= \int_0^{\infty} e^{-\tilde{\delta} r} \left|\mathbf{I}_L + \mathbf{B}_k r\right|^{-1} \mathrm{Tr}\left[\left(\mathbf{I}_L + \mathbf{B}_k r\right)^{-1} \mathbf{A}_k\right] dr, \end{aligned} \tag{18}$$

which can be simplified to (19) shown at the bottom of the next page, where $M = \min(K-1, L)$, and $\{\lambda_{k,l}\}_{l=1}^{M}$ and $\mathbf{V}_k \in \mathbb{C}^{L \times M}$ are the eigenvalues and the eigenvectors matrix of $\mathbf{B}_k$ respectively. The integral $I_{k,l}$ in (19) is evaluated in Appendix. As a result, we can also write $R_{\mathrm{sum}}^{\mathrm{UB}}$ in a closed-form. However, $\overline{\mathrm{SINR}}_k$ in (19) is a non-convex and non-differentiable function of the hybrid precoder, which makes the optimization problem in (8) difficult to solve.

B. A Closed-Form Expression for SLNR

An alternative approach to design the hybrid precoder is to consider SLNR. We derive a closed-form expression for $\overline{\mathrm{SLNR}}_k$. Interestingly, the derived $\overline{\mathrm{SLNR}}_k$ is a differentiable function of the hybrid precoder (as will be shown).

The average receive SLNR of the k^{th} user $\overline{\mathrm{SLNR}}_k$ is given by

$$\overline{\mathrm{SLNR}}_k = \mathbb{E}\left[\frac{\frac{L}{N_{\mathrm{T}}} \left|\mathbf{h}_k \mathbf{F}_{\mathrm{RF}} \mathbf{f}_{\mathrm{BB},k}\right|^2}{\frac{L}{N_{\mathrm{T}}} \sum_{\substack{i=1\\ i\neq k}}^{K} \left|\mathbf{h}_i \mathbf{F}_{\mathrm{RF}} \mathbf{f}_{\mathrm{BB},k}\right|^2 + \tilde{\delta}}\right]. \tag{20}$$

We know that $\sqrt{\frac{L}{N_{\mathrm{T}}}} \mathbf{h}_k \mathbf{F}_{\mathrm{RF}} \mathbf{f}_{\mathrm{BB},k} = \sum_{l=1}^{L} \alpha_{l,k} \mathbf{a}_{l,k}^H \mathbf{F}_{\mathrm{RF}} \mathbf{f}_{\mathrm{BB},k}$ which is a complex Gaussian random variable with zero-mean and variance of $\sum_{l=1}^{L} \left|\mathbf{a}_{l,k}^H \mathbf{F}_{\mathrm{RF}} \mathbf{f}_{\mathrm{BB},k}\right|^2$. Therefore, $v_1 =$

$\frac{L}{N_{\mathrm{T}}}\left|\mathbf{h}_k\mathbf{F}_{\mathrm{RF}}\mathbf{f}_{\mathrm{BB},k}\right|^2$ is an exponential random variable with mean value $\mu_{k,k}=\sum_{l=1}^{L}\left|\mathbf{a}_{l,k}^H\mathbf{F}_{\mathrm{RF}}\mathbf{f}_{\mathrm{BB},k}\right|^2$, and its PDF is given by [18]

$$f_{v_1}(v_1)=\frac{e^{-\frac{v_1}{\mu_{k,k}}}}{\mu_{k,k}},\ v_1>0. \tag{21}$$

In addition, $v_2=\frac{L}{N_{\mathrm{T}}}\sum_{\substack{i=1\\i\neq k}}^{K}\left|\mathbf{h}_i\mathbf{F}_{\mathrm{RF}}\mathbf{f}_{\mathrm{BB},k}\right|^2$ is a sum of independent exponential random variables with mean values of $\left\{\mu_{i,k}=\sum_{l=1}^{L}\left|\mathbf{a}_{l,i}^H\mathbf{F}_{\mathrm{RF}}\mathbf{f}_{\mathrm{BB},k}\right|^2\right\}_{\substack{i=1\\i\neq k}}^{K}$, which results in a hypo-exponential random variable with a PDF given by [18]

$$f_{v_2}(v_2)=\sum_{\substack{i=1\\i\neq k}}^{K}\frac{t_i e^{-\frac{v_2}{\mu_{i,k}}}}{\mu_{i,k}},\ v_2>0, \tag{22}$$

where $t_i=\prod_{\substack{m=1\\m\neq i,\,m\neq k}}^{K}\frac{\mu_{i,k}}{\mu_{i,k}-\mu_{m,k}}$. Therefore, we can obtain the joint moment generating function $M_{v_1,v_2}(s,r)$ of v_1 and v_2 as

$$\begin{aligned}M_{v_1,v_2}(s,r)&=e^{-\tilde{\delta}r}\int_0^\infty\frac{e^{-v_1\left(\frac{1}{\mu_{k,k}}-s\right)}}{\mu_{k,k}}dv_1\\&\quad\times\sum_{\substack{i=1\\i\neq k}}^{K}\int_0^\infty\frac{t_i e^{-v_2\left(\frac{1}{\mu_{i,k}}-r\right)}}{\mu_{i,k}}dv_2\\&=e^{-\tilde{\delta}r}\frac{1}{1-\mu_{k,k}s}\sum_{\substack{i=1\\i\neq k}}^{K}\frac{t_i}{1-\mu_{i,k}r}.\end{aligned} \tag{23}$$

Using (16), we can evaluate $\overline{\mathrm{SLNR}}_k$ as

$$\begin{aligned}\overline{\mathrm{SLNR}}_k&=\int_0^\infty\left[\frac{\partial}{\partial s}e^{-\tilde{\delta}r}\frac{1}{1-\mu_{k,k}s}\sum_{\substack{i=1\\i\neq k}}^{K}\frac{t_i}{1+\mu_{i,k}r}\right]_{s=0}dr\\&=\mu_{k,k}\sum_{\substack{i=1\\i\neq k}}^{K}t_i\int_0^\infty\frac{e^{-\tilde{\delta}r}}{1+\mu_{i,k}r}dr\\&=-\mu_{k,k}\sum_{\substack{i=1\\i\neq k}}^{K}\frac{t_i}{\mu_{i,k}}e^{\frac{\tilde{\delta}}{\mu_{i,k}}}\mathrm{Ei}\left(-\frac{\tilde{\delta}}{\mu_{i,k}}\right),\end{aligned} \tag{24}$$

where $\mathrm{Ei}(x)=-\int_{-x}^{\infty}\frac{e^{-t}}{t}dt$ is the exponential integral. We can also get a lower bound on $\overline{\mathrm{SLNR}}_k$ as

$$\begin{aligned}\overline{\mathrm{SLNR}}_k&\geq\frac{\mathbb{E}\left[\frac{L}{N_{\mathrm{T}}}\left|\mathbf{h}_k\mathbf{F}_{\mathrm{RF}}\mathbf{f}_{\mathrm{BB},k}\right|^2\right]}{\mathbb{E}\left[\frac{L}{N_{\mathrm{T}}}\sum_{i\neq k}\left|\mathbf{h}_i\mathbf{F}_{\mathrm{RF}}\mathbf{f}_{\mathrm{BB},k}\right|^2+\tilde{\delta}\right]}\\&=\frac{\sum_{l=1}^{L}\left|\mathbf{a}_{l,k}^H\mathbf{F}_{\mathrm{RF}}\mathbf{f}_{\mathrm{BB},k}\right|^2}{\sum_{\substack{i=1\\i\neq k}}^{K}\sum_{l=1}^{L}\left|\mathbf{a}_{l,i}^H\mathbf{F}_{\mathrm{RF}}\mathbf{f}_{\mathrm{BB},k}\right|^2+\tilde{\delta}}\triangleq\overline{\mathrm{SLNR}}_k^{\mathrm{LB}},\end{aligned} \tag{25}$$

where the inequality holds since the numerator and denominator are independent and $\mathbb{E}\left[\frac{1}{x}\right]\geq\frac{1}{\mathbb{E}[x]}$ by Jensen's inequality.

C. Optimizing Algorithm

Using $\overline{\mathrm{SLNR}}_k^{\mathrm{LB}}$, we obtain the baseband precoder as a function of the RF precoder. To decouple the design of the baseband precoders $\{\mathbf{f}_{\mathrm{BB},k}\}$, we relax the power constraint to $\left\|\mathbf{F}_{\mathrm{RF}}\mathbf{f}_{\mathrm{BB},k}\right\|^2=1$, which also satisfies $\left\|\mathbf{F}_{\mathrm{RF}}\mathbf{F}_{\mathrm{BB}}\right\|_{\mathrm{F}}^2=K$. Applying the new power constraint into $\overline{\mathrm{SLNR}}_k^{\mathrm{LB}}$, we get

$$\begin{aligned}\overline{\mathrm{SLNR}}_k^{\mathrm{LB}}&=\frac{\sum_{l=1}^{L}\left|\mathbf{a}_{l,k}^H\mathbf{F}_{\mathrm{RF}}\mathbf{f}_{\mathrm{BB},k}\right|^2}{\sum_{\substack{i=1\\i\neq k}}^{K}\sum_{l=1}^{L}\left|\mathbf{a}_{l,i}^H\mathbf{F}_{\mathrm{RF}}\mathbf{f}_{\mathrm{BB},k}\right|^2+\tilde{\delta}\left|\mathbf{F}_{\mathrm{RF}}\mathbf{f}_{\mathrm{BB},k}\right|^2}\\&=\frac{\mathbf{f}_{\mathrm{BB},k}^H\left(\mathbf{F}_{\mathrm{RF}}^H\sum_{l=1}^{L}\mathbf{a}_{l,k}\mathbf{a}_{l,k}^H\mathbf{F}_{\mathrm{RF}}\right)\mathbf{f}_{\mathrm{BB},k}}{\mathbf{f}_{\mathrm{BB},k}^H\left(\mathbf{F}_{\mathrm{RF}}^H\sum_{\substack{i=1\\i\neq k}}^{K}\sum_{l=1}^{L}\mathbf{a}_{l,i}\mathbf{a}_{l,i}^H\mathbf{F}_{\mathrm{RF}}+\tilde{\delta}\mathbf{F}_{\mathrm{RF}}^H\mathbf{F}_{\mathrm{RF}}\right)\mathbf{f}_{\mathrm{BB},k}}.\end{aligned} \tag{26}$$

Using generalized eigenvector decomposition, we obtain $\mathbf{f}_{\mathrm{BB},k}$ maximizing $\overline{\mathrm{SLNR}}_k^{\mathrm{LB}}$ as in (27) shown at the bottom of the page.

Now, we propose a suboptimal gradient ascent algorithm to design the RF precoder $\mathbf{F}_{\mathrm{RF}}$. Note that $\overline{\mathrm{SLNR}}_k$ in (24) is differentiable while $\overline{\mathrm{SINR}}_k$ in (19) is not. Therefore, we use the gradient of $\sum_{k=1}^{K}\overline{\mathrm{SLNR}}_k$ to maximize $R_{\mathrm{sum}}^{\mathrm{UB}}$. The gradient $\nabla_{\mathbf{F}_{\mathrm{RF}}}$ of $\sum_{k=1}^{K}\overline{\mathrm{SLNR}}_k$ with respect to the RF precoder $\mathbf{F}_{\mathrm{RF}}$ is obtained (after mathematical manipulations) as in (28) shown at the bottom of the next page, where

$$\nabla_{\mathbf{F}_{\mathrm{RF}}}(\mu_{i,k})=\sum_{l=1}^{L}\mathbf{a}_{l,i}\mathbf{a}_{l,i}^H\mathbf{F}_{\mathrm{RF}}\mathbf{f}_{\mathrm{BB},k}\mathbf{f}_{\mathrm{BB},k}^H, \tag{29}$$

$$\nabla_{\mathbf{F}_{\mathrm{RF}}}(t_i)=t_i\sum_{\substack{m=1\\m\neq i,\,m\neq k}}^{K}\frac{\mu_{i,k}\nabla_{\mathbf{F}_{\mathrm{RF}}}(\mu_{m,k})-\mu_{m,k}\nabla_{\mathbf{F}_{\mathrm{RF}}}(\mu_{i,k})}{\mu_{i,k}^2-\mu_{i,k}\mu_{m,k}}. \tag{30}$$

Using the gradient $\nabla_{\mathbf{F}_{\mathrm{RF}}}$ in (28), we obtain the RF precoder $\mathbf{F}_{\mathrm{RF}}$ by Algorithm 1, where P_{RF} is the number of iterations, and the updating rule is solved by a backtracking line search over the step size α [20]. We initialize the RF precoder as the proposed ZF RF precoder if it is feasible ($N_{\mathrm{T}}>(K-1)L$ and $N_{\mathrm{RF}}\geq 2K$). If not, we initialize the RF precoder randomly while satisfying the unit modulus constraint $\left|\mathbf{F}_{\mathrm{RF}}(m,n)\right|=1\forall m,n$. Note that the updating rule in Algorithm 1 is done based on $R_{\mathrm{sum}}^{\mathrm{UB}}$, which ensures an increase in $R_{\mathrm{sum}}^{\mathrm{UB}}$ in each iteration, and hence it ensures the convergence of the algorithm. Note that we have a closed-form for $R_{\mathrm{sum}}^{\mathrm{UB}}$ thanks to the closed-form SINR in (19).

V. Eigenvector-SLNR Hybrid Precoder

In this section, we present the Eigenvector-SLNR (EV-SLNR) hybrid precoder, which we consider as our benchmark design. Specifically, we develop EV-SLNR hybrid precoder based on [10], [11], [21] with some modifications to satisfy the unit modulus constraint and the power constraint.

$$\overline{\mathrm{SINR}}_k=\mathbf{f}_{\mathrm{BB},k}^H\mathbf{F}_{\mathrm{RF}}^H\mathbf{A}_{\mathrm{T},k}\mathbf{V}_k\mathrm{diag}\left(\left\{\underbrace{\int_0^\infty\frac{e^{-\tilde{\delta}r}dr}{(1+\lambda_{k,l}r)\prod_{m=1}^{M}(1+\lambda_{k,m}r)}}_{I_{k,l}}\right\}_{l=1}^{M}\right)\mathbf{V}_k^H\mathbf{A}_{\mathrm{T},k}^H\mathbf{F}_{\mathrm{RF}}\mathbf{f}_{\mathrm{BB},k}. \tag{19}$$

$$\mathbf{f}_{\mathrm{BB},k}=\frac{\boldsymbol{\mathcal{E}}_{\max}\left[\left(\mathbf{F}_{\mathrm{RF}}^H\sum_{\substack{i=1\\i\neq k}}^{K}\sum_{l=1}^{L}\mathbf{a}_{l,i}\mathbf{a}_{l,i}^H\mathbf{F}_{\mathrm{RF}}+\tilde{\delta}\mathbf{F}_{\mathrm{RF}}^H\mathbf{F}_{\mathrm{RF}}\right)^{-1}\mathbf{F}_{\mathrm{RF}}^H\sum_{l=1}^{L}\mathbf{a}_{l,k}\mathbf{a}_{l,k}^H\mathbf{F}_{\mathrm{RF}}\right]}{\left\|\mathbf{F}_{\mathrm{RF}}\boldsymbol{\mathcal{E}}_{\max}\left[\left(\mathbf{F}_{\mathrm{RF}}^H\sum_{\substack{i=1\\i\neq k}}^{K}\sum_{l=1}^{L}\mathbf{a}_{l,i}\mathbf{a}_{l,i}^H\mathbf{F}_{\mathrm{RF}}+\tilde{\delta}\mathbf{F}_{\mathrm{RF}}^H\mathbf{F}_{\mathrm{RF}}\right)^{-1}\mathbf{F}_{\mathrm{RF}}^H\sum_{l=1}^{L}\mathbf{a}_{l,k}\mathbf{a}_{l,k}^H\mathbf{F}_{\mathrm{RF}}\right]\right\|}. \tag{27}$$

Algorithm 1 Hybrid precoder design for average sum rate maximization

Initialization: Obtain $\mathbf{F}_{\mathrm{RF}}^{(0)}$ as the proposed ZF RF precoder if it is feasible. If not, obtain $\mathbf{F}_{\mathrm{RF}}^{(0)}$ randomly while satisfying the unit modulus constraint. Then, obtain $\mathbf{F}_{\mathrm{BB}}^{(0)}$ using (27).
while $p \leq P$ (or any other appropriate stopping criterion)
  Calculate the gradient $\nabla_{\mathbf{F}_{\mathrm{RF}}}^{(p)}$ using (28)–(30) with $\mathbf{F}_{\mathrm{BB}} = \mathbf{F}_{\mathrm{BB}}^{(p)}$.
  Updating rule:

$$\left[\mathbf{F}_{\mathrm{RF}}^{(p+1)}, \mathbf{F}_{\mathrm{BB}}^{(p+1)}, \alpha\right] = \underset{\mathbf{F}_{\mathrm{RF}}, \mathbf{F}_{\mathrm{BB}}, \alpha}{\arg\max} \; R_{\mathrm{sum}}^{\mathrm{UB}}\left(\mathbf{F}_{\mathrm{RF}}, \mathbf{F}_{\mathrm{BB}}\right),$$
$$\text{s.t.} \quad \mathbf{F}_{\mathrm{RF}} = e^{j\angle\left(\mathbf{F}_{\mathrm{RF}}^{(p)} + \alpha \nabla_{\mathbf{F}_{\mathrm{RF}}}^{(p)}\right)},$$
$$\mathbf{F}_{\mathrm{BB}} \text{ as in (27).}$$

  $p = p + 1$.
end while
Output: $\mathbf{F}_{\mathrm{RF}}^{(P+1)}$, $\mathbf{F}_{\mathrm{BB}}^{(P+1)}$.

As proposed in [10], [21], the RF precoder $\mathbf{F}_{\mathrm{RF}}$ is obtained using the principal eigenvectors of $\left\{\sum_{l=1}^{L} \mathbf{a}_{l,k}\mathbf{a}_{l,k}^{H}\right\}_{k=1}^{K}$ as

$$\mathbf{F}_{\mathrm{RF}} = \left[e^{j\angle \boldsymbol{\mathcal{E}}_{\max}\left[\sum_{l=1}^{L} \mathbf{a}_{l,1}\mathbf{a}_{l,1}^{H}\right]}, \ldots, e^{j\angle \boldsymbol{\mathcal{E}}_{\max}\left[\sum_{l=1}^{L} \mathbf{a}_{l,K}\mathbf{a}_{l,K}^{H}\right]}\right], \quad (31)$$

where we use only the phases of the principal eigenvectors to satisfy the unit modulus constraint. As proposed in [11], the baseband precoder $\mathbf{f}_{\mathrm{BB},k}$ is designed to maximize $\overline{\mathrm{SLNR}}_k^{\mathrm{LB}}$. In [11], the power constraint $\|\mathbf{F}_{\mathrm{RF}}\mathbf{f}_{\mathrm{BB},k}\|^2 = 1$ is applied after obtaining $\mathbf{f}_{\mathrm{BB},k}$. On the contrary, we apply the power constraint into $\overline{\mathrm{SLNR}}_k^{\mathrm{LB}}$ before obtaining $\mathbf{f}_{\mathrm{BB},k}$. Therefore, our closed-form baseband precoder in (27) is more accurate than that in [11]. The main advantage of EV-SLNR hybrid precoder is that the RF precoder and the baseband precoder can be written in closed-forms as in (27) and (31). However, EV-SLNR hybrid precoder utilizes only K RF chains out of the available N_{RF} RF chains, which results in some performance loss.

VI. Numerical Results

We evaluate the performance of the proposed hybrid precoder designs and compare them with the performance of EV-SLNR hybrid precoder by means of Monte-Carlo simulations. Note that the proposed SINR-SLNR hybrid precoder is different from EV-SLNR hybrid precoder in the design of the RF precoder. EV-SLNR hybrid precoder utilizes only K RF chains out of the available N_{RF} RF chains. On the contrary, the proposed SINR-SLNR hybrid precoder utilizes the available N_{RF} RF chains.

Regarding the simulation setup, we assume that the transmitter has 20 antennas ($N_{\mathrm{T}} = 20$), and we have 4 users ($K = 4$). The number of RF chains N_{RF} will be an adjustable parameter. All channels follow the mmWave channel model described in subsection II-B with 6 propagation paths ($L = 6$), where the channel gains $\{\alpha_{l,k}\}$ are zero-mean and unit-variance complex Gaussian random variables, and the angles of departure $\{\varphi_{l,k}\}$ are uniformly-distributed within $[0\ 2\pi)$.

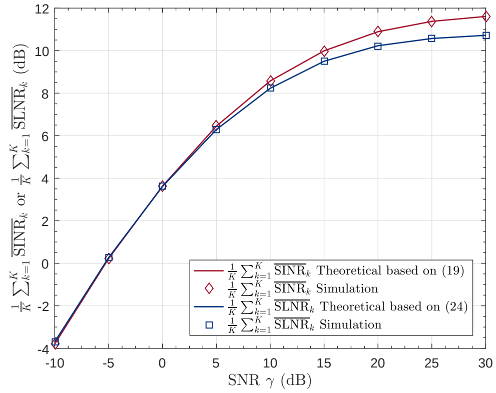

Fig. 2. Verification of our closed-form expressions of SINR in (19) and SLNR in (24) with values obtained by simulation with $N_{\mathrm{RF}} = 4$.

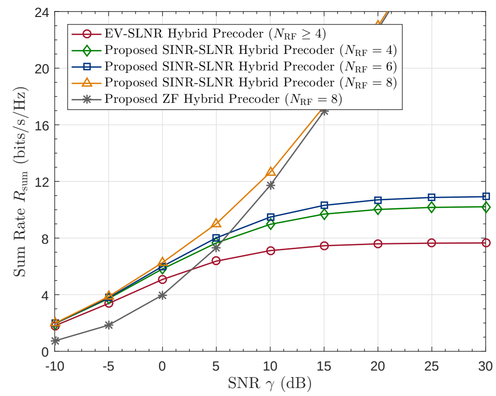

Fig. 3. Achievable sum rate R_{sum} as a function of transmit SNR γ with $K = 4$ and different numbers of N_{RF}.

Fig 2. shows the average SINR ($\frac{1}{K}\sum_{k=1}^{K}\overline{\mathrm{SINR}}_k$) and the average SLNR ($\frac{1}{K}\sum_{k=1}^{K}\overline{\mathrm{SINR}}_k$) versus transmit SNR γ with $N_{\mathrm{RF}} = 4$. We observe that the closed-form expressions in (19) and (24) exactly match the corresponding values obtained by simulation, which verifies our closed-form expressions. We also observe that the average SLNR gives a good approximation to the average SINR, which enables us to use the gradient in (28) of the average SLNR to maximize the sum rate (as used in Algorithm 1).

Fig 3. shows the achievable sum rate R_{sum} as a function of the transmit SNR γ with different numbers of RF chains.With $N_{\mathrm{RF}} = 4$, the proposed ZF hybrid precoder is infeasible. On the other hand, the proposed SINR-SLNR hybrid precoderand EV-SLNR hybrid precoder are feasible. The proposed SINR-SLNR hybrid precoder outperforms EV-SLNR hybrid precoder specifically at moderate and high SNRs. The sum-rate gap between the proposed SINR-SLNR hybrid precoder and EV-SLNR hybrid precoder increases as we increase N_{RF} to 6 and 8. The reason is that EV-SLNR hybrid precoder utilizes only

$$\nabla_{\mathbf{F}_{\mathrm{RF}}} = \sum_{k=1}^{K}\sum_{\substack{i=1 \\ i\neq k}}^{K}\left[\left(\frac{\mu_{k,k}\nabla_{\mathbf{F}_{\mathrm{RF}}}(\mu_{i,k}) - \mu_{i,k}\nabla_{\mathbf{F}_{\mathrm{RF}}}(\mu_{k,k})}{\mu_{i,k}^2} t_i - \frac{\mu_{k,k}}{\mu_{i,k}}\nabla_{\mathbf{F}_{\mathrm{RF}}}(t_i)\right) e^{\frac{\tilde{\delta}}{\mu_{i,k}}}\,\mathrm{Ei}\left(-\frac{\tilde{\delta}}{\mu_{i,k}}\right)\right.$$
$$\left. + t_i \frac{\mu_{k,k}}{\mu_{i,k}} \frac{\tilde{\delta} e^{\frac{\tilde{\delta}}{\mu_{i,k}}}\,\mathrm{Ei}\left(-\frac{\tilde{\delta}}{\mu_{i,k}}\right) + \mu_{i,k}}{\mu_{i,k}^2}\nabla_{\mathbf{F}_{\mathrm{RF}}}(\mu_{i,k})\right]. \quad (28)$$

K RF chains out of the available $N_{\rm RF}$ RF chain, while the proposed SINR-SLNR hybrid precoder utilizes the available $N_{\rm RF}$ RF chains. With $N_{\rm RF} = 8$, the proposed ZF hybrid precoder is feasible, and it outperforms EV-SLNR at high SNRs since nulling the interference is the optimal strategy at high SNRs. However, the proposed ZF hybrid precoder achieves the lowest sum rate at low SNRs since the system is power-limited and nulling the interference is not the optimal strategy at low SNRs. We also observe that with the same number of RF chains the proposed SINR-SLNR hybrid precoder outperforms the proposed ZF hybrid precoder at low and moderate SNRs on the expense of higher computational complexity.

VII. Conclusion

For mmWave multiuser downlink systems, the use of hybrid precoders and partial channel knowledge is more practical than that of fully digital precoders and/or full channel knowledge. We developed three hybrid precoders (ZF, SINR-SLNR, and EV-SLNR) based on partial channel knowledge in contrast to the full channel knowledge required in the existing approaches. The interference nulling of ZF hybrid precoder is feasible with partial channel knowledge if necessary conditions on the numbers of transmit antennas and RF chains are satisfied, which is more demanding than that with full channel knowledge. For the scenarios not satisfying the necessary conditions of ZF, we proposed SINR-SLNR hybrid precoder. We also developed EV-SLNR hybrid precoder (a modification of the existing approaches to fit to the partial channel knowledge scenario) as a benchmark. When ZF is not feasible, there will be interference and hence the sum-rate performance of SINR-SLNR and EV-SLNR hybrid precoders would not linearly grow with SNR at high SNRs. However, the SINR-SLNR hybrid precoder outperforms the EV-SLNR hybrid precoder and its sum-rate performance is also enhanced by increasing the number of RF chains while it is not the case for the EV-SLNR hybrid precoder. When ZF is feasible, the sum-rate performance of the ZF hybrid precoder is substantially better at high SNRs, but worse at low SNRs than those of the other schemes. With the same number of RF chains, the proposed SINR-SLNR hybrid precoder yields better sum-rate performance than all the other schemes on the expense of higher computational complexity.

Appendix: Evaluating The Integral $I_{k,l}$ in (19)

Defining $\mu_{k,l} = \frac{1}{\lambda_{k,l}}$, the integral $I_{k,l}$ in (19) can be written as $I_{k,l} = \mu_{k,l}\left(\prod_{m=1}^{M}\mu_{k,m}\right)\tilde{I}_{k,l}$, where

$$\begin{aligned}\tilde{I}_{k,l} &= \int_0^\infty \frac{e^{-\tilde{\delta}r}dr}{(r+\mu_{k,l})\prod_{m=1}^{M}(r+\mu_{k,m})}\\ &= \int_0^\infty \left(\frac{a_{k,l}e^{-\tilde{\delta}r}}{(r+\mu_{k,l})^2} + \frac{b_{k,l}e^{-\tilde{\delta}r}}{(r+\mu_{k,l})} + \sum_{m=1,\, m\neq l}^{M}\frac{c_{k,m}e^{-\tilde{\delta}r}}{(r+\mu_{k,m})}\right)dr\\ &= a_{k,l}\left(\tilde{\delta}e^{\mu_{k,l}\tilde{\delta}}\mathrm{Ei}\left(-\mu_{k,l}\tilde{\delta}\right) + \frac{1}{\mu_{k,l}}\right) - b_{k,l}e^{\mu_{k,l}\tilde{\delta}}\mathrm{Ei}\left(-\mu_{k,l}\tilde{\delta}\right)\\ &\quad - \sum_{m=1,\, m\neq l}^{M} c_{k,m}e^{\mu_{k,m}\tilde{\delta}}\mathrm{Ei}\left(-\mu_{k,m}\tilde{\delta}\right),\end{aligned} \tag{32}$$

where $\mathrm{Ei}(x) = -\int_{-x}^{\infty}\frac{e^{-t}}{t}dt$ is the exponential integral, and the partial fraction coefficients are obtained as $a_{k,l} = \frac{1}{\prod_{n=1,\, n\neq l}^{M}(\mu_{k,n}-\mu_{k,l})}$, $b_{k,l} = \left[\frac{\partial}{\partial r}\frac{1}{\prod_{n=1,\, n\neq l}^{M}(r+\mu_{k,n})}\right]_{r=-\mu_{k,l}}$, and $c_{k,m} = \frac{1}{(\mu_{k,l}-\mu_{k,m})\prod_{n=1,\, n\neq m}^{M}(\mu_{k,n}-\mu_{k,m})}$.

References

[1] T. Rappaport, S. Sun, R. Mayzus, H. Zhao, Y. Azar, K. Wang, G. Wong, J. Schulz, M. Samimi, and F. Gutierrez, "Millimeter wave mobile communications for 5G cellular: It will work!" *IEEE Access*, vol. 1, pp. 335–349, May 2013.

[2] O. Ayach, R. Heath, S. Abu-Surra, S. Rajagopal, and Z. Pi, "Low complexity precoding for large millimeter wave MIMO systems," in *Proc. IEEE ICC 2012*, Jun. 2012, pp. 3724–3729.

[3] Z. Xu, S. Han, Z. Pan, and C. L. I, "Alternating beamforming methods for hybrid analog and digital MIMO transmission," in *Proc. IEEE ICC 2015*, Jun. 2015, pp. 1595–1600.

[4] W. Ni, X. Dong, and W. S. Lu, "Near-optimal hybrid processing for massive mimo systems via matrix decomposition," *IEEE Trans. Signal Process.*, vol. 65, no. 15, pp. 3922–3933, Aug. 2017.

[5] X. Yu, J. C. Shen, J. Zhang, and K. B. Letaief, "Alternating minimization algorithms for hybrid precoding in millimeter wave MIMO systems," *IEEE J. Sel. Topics Signal Process.*, vol. 10, no. 3, pp. 485–500, Apr. 2016.

[6] A. Alkhateeb, R. W. Heath, and G. Leus, "Achievable rates of multi-user millimeter wave systems with hybrid precoding," in *Proc. IEEE ICCW 2015*, Jun. 2015, pp. 1232–1237.

[7] A. Alkhateeb, G. Leus, and R. W. Heath, "Limited feedback hybrid precoding for multi-user millimeter wave systems," *IEEE Trans. Wireless Commun.*, vol. 14, no. 11, pp. 6481–6494, Nov. 2015.

[8] D. H. N. Nguyen, L. B. Le, and T. Le-Ngoc, "Hybrid MMSE precoding for mmWave multiuser MIMO systems," in *IEEE ICC 2016*, May 2016, pp. 1–6.

[9] A. Alkhateeb, O. El Ayach, G. Leus, and R. Heath, "Hybrid precoding for millimeter wave cellular systems with partial channel knowledge," in *Proc. ITA 2013, 2013*, Feb. 2013, pp. 1–5.

[10] A. Alkhateeb, G. Leus, and R. W. Heath, "Multi-layer precoding for full-dimensional massive mimo systems," in *Proc. IEEE Asilomar Conf. Signal, Syst. Comput. 2014*, Nov. 2014, pp. 815–819.

[11] M. Dai and B. Clerckx, "Multiuser millimeter wave beamforming strategies with quantized and statistical CSIT," *IEEE Trans. Wireless Commun.*, 2017, doi:10.1109/TWC.2017.2737009.

[12] J. Wang, P. Ding, M. Zoltowski, and D. Love, "Space-time coding and beamforming with partial channel state information," in *Proc. IEEE GLOBECOM 2005*, vol. 5, Dec. 2005, pp. 3149–3153.

[13] Y. Ramadan, A. Ibrahim, and M. Khairy, "Minimum outage RF beamforming for millimeter wave MISO-OFDM systems," in *Proc. IEEE WCNC 2015*, Mar. 2015, pp. 557–561.

[14] S.-K. Yong, P. Xia, and A. Valdes-Garcia, *60 GHz technology for Gbps WLAN and WPAN: From theory to practice*. Wiley, 2010.

[15] H. Xu, V. Kukshya, and T. S. Rappaport, "Spatial and temporal characteristics of 60-GHz indoor channels," *IEEE J. Sel. Areas Commun.*, vol. 20, no. 3, pp. 620–630, Apr. 2002.

[16] M. R. Akdeniz, Y. Liu, M. K. Samimi, S. Sun, S. Rangan, T. S. Rappaport, and E. Erkip, "Millimeter wave channel modeling and cellular capacity evaluation," *IEEE J. Sel. Areas Commun.*, vol. 32, no. 6, pp. 1164–1179, Jun. 2014.

[17] X. Zhang, A. F. Molisch, and S.-Y. Kung, "Variable-phase-shift-based RF-baseband codesign for MIMO antenna selection," *IEEE Trans. Signal Process.*, vol. 53, no. 11, pp. 4091–4103, Nov. 2005.

[18] H. Stark and J. Woods, *Probability, statistics, and random processes for engineers*. Prentice Hall, 2012.

[19] J. Magnus, "The exact moments of a ratio of quadratic forms in normal variables," *Annales d'Economie et de Statistique 4*, no. 4, pp. 95–109, Oct./Dec. 1986.

[20] S. Boyd and L. Vandenberghe, *Convex Optimization*. Cambridge, UK: Cambridge University Press, 2004.

[21] L. Liang, Y. Dai, W. Xu, and X. Dong, "How to approach zero-forcing under RF chain limitations in large mmwave multiuser systems?" in *IEEE/CIC ICCC 2014*, Oct. 2014, pp. 518–522.